Research Journal in Civil, Industrial and Mechanical Engineering
ISSN: 3079-2630
DOI: https://doi.org/10.61424/rjcime.v3i1.943
Journal Homepage: https://bluemarkpublishers.com/index.php/RJIEE

RJCIME
BLUEMARK PUBLISHERS

| RESEARCH ARTICLE

Characterization of Phase Change Materials for Enhancing Thermal Energy Storage in District Cooling Systems

Sharmin Akter[1] ✉ Md. Anowar Hossain[2], Hasan M. M. Afroz[3]
[12]Department of Mechanical Engineering, Dhaka University of Engineering & Technology (DUET), Gazipur, Bangladesh
[3]Department of Materials and Metallurgical Engineering, Dhaka University of Engineering & Technology (DUET), Gazipur, Bangladesh
Corresponding Author: Sharmin Akter, **E-mail**: islamsharmin991.bd@gmail.com

| ABSTRACT
Thermal energy storage is a vital measure for mitigating peak electricity demand in district cooling systems with the increasing demand for cooling worldwide. The present study has experimentally investigated the potential of water–ethylene glycol mixtures as cold storage media for district cooling thermal energy storage, focussing on the charging and discharging characteristics of the cold storage tank. A thermal energy storage tank with a vapor-compression chiller was used to test six mixtures containing 0%, 10%, 20%, 30%, 40% and 50% ethylene glycol by mass. The system performance was assessed by measuring the reservoir temperature, load-side temperature, charging time, electrical energy consumption, and discharging time. The experiments revealed that ethylene glycol had positive effects on sub-zero charging. Pure water was cooled from 19.1 °C to 2.0 °C in 14.51 min with 0.64 kWh energy consumption, while the 80:20 and 70:30 water–ethylene glycol mixtures reached −6.0 °C and −9.0 °C with 1.13 and 1.54 kWh, respectively. The mixture with 90% of LiCl solution and 10% of LiCl solid gave the longest discharge time, of 191.23 min while the 80:20 mixture gave a balancing charging and discharging behaviour. The results show that water–ethylene glycol mixtures are potentially optimal as practical cold storage media for district cooling (DC) thermal storage applications.

| KEYWORDS

Phase change material; District cooling system; Thermal energy storage; Water–ethylene glycol; Latent heat.

| ARTICLE INFORMATION

ACCEPTED: 15 May 2026 **PUBLISHED:** 13 July 2026 **DOI:** https://doi.org/10.61424/rjcime.v3i1.943

1. Introduction

The rapid growth of global cooling demand has become one of the major challenges for modern energy systems, especially in hot and humid regions where air-conditioning loads dominate building electricity consumption during peak hours. Space cooling is one of the most rapidly increasing energy demand in buildings; the world's energy use for cooling has more than tripled since 1990, which is putting a strain on electricity networks, energy bills, and greenhouse gas emissions [Bandyopadhyay, 2022], [Waite, 2017]. Air conditioners and electric fans are also reported to consume almost 20% of the total electricity used in buildings and have also shown their significant impact on electricity consumption globally on a large scale [Duan, 2025]. The demand is further exacerbated by urbanization, increasing income, climate change and more extreme hot events. Cooling load is often at its highest in the peak hours of the day in many cities, right at the time that the electricity network is under stress [Mohamed, 2025]. It is therefore a practical solution to use district cooling systems (DCSs), which produce chilled water at a

central plant and send it to various buildings via insulated pipeline networks. This configuration may be more efficient in equipment use, operation and control, and plant efficiency than a stand-alone building cooling system [Liang, 2016], [Al-Nini, 2023]. However, the peak cooling demand, variation in electricity tariff, chilled-water temperature limits and the requirement for flexibility in plant operation are still significant influences on DCS operation [Oró, 2012], [Liu, 2012].

Thermal energy storage (TES) has been shown to be an effective method to enhance flexibility of DCS operation by decoupling the time of cooling production with the time of cooling use. During periods of reduced tariff or off-peak night time, chillers are able to charge the storage system and during peak-load periods, the chilled water can be discharged [Gao, 2026], [Tang, 2023]. This approach can decrease peak electric load, achieve chiller operating stability, and promote grid-friendly cooling operation. Many studies have been performed to prove that the application of thermal storage under commercial operating conditions would reduce the peak cooling load and move load from peak to off-peak periods [Guillén-Lambea, 2021], [McKenna, 2021]. The conventional sensible storage with chilled water is simple and mature, but it is necessary to make large tank volume due to the energy stored only by the temperature difference. The latent heat storage with phase change materials (PCMs), on the other hand, can store and release huge quantities of heat within a small temperature range while the material is melting and solidifying [Mao, 2025], [Dzhonova-Atanasova, 2022], [Heier, 2015]. The near-isothermal operation is particularly interesting for cooling applications where it gives a stable chilled-water delivery during discharge. Recent DCS studies have also demonstrated that to realize the efficient thermal and exergy performance, storage systems need to be appropriately matched to the chilled-water operating range, which is typically between the supply and return water temperatures of 5 °C and 12 °C, respectively [Shao, 2023]. TES design also has impact at the sustainability level both in terms of operation energy and life-cycle environmental impact [Vielma, 2026].

There are three groups of PCMs are generally used in TES cooling systems, organic, inorganic and eutectic materials with their merits and demerits. Organic PCMs are extensively studied because of their predictable phase change properties, low corrosive risk and chemical stability [Senobar, 2026], [Samykano, 2022]. Many of them possess phase change temperatures that are in or around the 5-30 °C range, making them suitable for construction for cooling and chilled water [Irshad, 2025]. But they tend to be slow to charge and discharge because of their low conductivity. Salt hydrates and chloride salts are inorganic PCMs that can offer high volumetric storage density and large operating temperature range, but may experience supercooling, phase separation, corrosion and cycling instability [Han, 2020], [Choo, 2022]. Other materials of interest include eutectic mixtures and aqueous solutions, which also have the property of having a freezing point or melting point which can be varied with composition, for near zero or sub-zero cold storage [Brancato, 2017]. Ice storage is high energy density, but generally requires sub-zero charging temperatures, which may lead to a decrease in chiller's coefficient of performance and increase in system complexity [Pereira, 2016]. Thus, a proper cold storage medium for DCS should not only have high storage capacity but also should have a reasonable charging/discharging range with minimal energy loss [Oró, 2012].

There has been significant work on PCM for TES for cooling application previously. The following type of encapsulated PCM tanks, ice-storage system, paraffin-based material, salt hydrates and pilot-scale TES configurations have been investigated under various conditions. The research in [Shao, 2023] demonstrated that an organic PCM mixture with the phase-change temperature near the DCS chilled water storage temperature can be better than conventional chilled water and encapsulated ice in the storage capacity. The result validates the importance of adapting the cooling-network conditions to the PCM storage conditions. Pilot-scale studies in [Zhao, 2010] also revealed that the PCM behavior in small scale laboratory samples can be different from larger scale due to the effects of sample size, thermal mass, and boundary conditions on melting and solidification. In solar absorption cooling, other cooling-system studies have demonstrated that the storage volume of the system can be decreased with the use of PCM [Hirmiz, 2018] and in space-cooling applications, the peak electrical demand can be also reduced [Farah, 2019]. The studies of salt hydrate and inorganic PCM also indicate problems of supercooling, incongruent melting and phase instability that hinder long-term use [Xie, 2017]. The results indicate that material selection should not rely exclusively on the latent heat, but also on the reversibility, the thermal stability and the compatibility with the actual conditions of the system.

Other key aspects in the development of a reliable cold storage system with PCM's are heat transfer enhancement and material characterization [Liu, 2025], [Li, 2024]. The intrinsic thermal resistivities of many PCMs are low, causing the melting or solidification process to be incomplete when charging and discharging under limited conditions [Liu, 2024]. In order to solve this problem, previous works have investigated the use of nanoparticle additives, composite PCMs, metal structures, and finned geometries. Nano-enhanced organic eutectic PCMs have been found that enhance the thermal conductivity with good phase change behavior on cycling [Jacob, 2022]. However, there are concerns about filler dispersion, long-term stability, and cost while using carbon-based additives to enhance thermal response and to reduce supercooling [He, 2019]. Structural enhancement of the latent heat capacity has been achieved by composite PCM research without compromising the heat storage and release behaviour [Trigui, 2013]. Finned TES designs may also help to decrease melting time because of the enhanced internal heat exchange [Zhang, 2020]. Techniques for enhancing however can limit the effective storage density if inactive support materials, shells or additives take up too much space. Therefore, application of appropriate characterization techniques, such as DSC, thermal conductivity measurement, density analysis, supercooling evaluation and thermal cycling tests, are key prerequisites before any system application. PCM reviews are also found across the board which highlight the limited characterization of the PCM in the liquid phase, particularly of real discharge performance [Yang, 2021], [Islam, 2024].

Water–ethylene glycol (W–EG) systems have been successfully employed in cooling and refrigeration practice as heat-transfer fluids, secondary refrigerants, and brine solutions for sub-zero applications [Selvnes, 2021], [Rashid, 2023]. This is the reason that ethylene glycol–water brine is often circulated through heat exchangers or coils to freeze and melt ice in an ice-storage tank, so that the ethylene glycol–water brine can be circulated below the freezing temperature of pure water [Ukpe, 2022]. The effect of freezing point depression of the W–EG mixtures is well known and the freezing temperature can be modified by varying the EG concentration [Gabas, 2003]. W-EG mixtures are technically interesting not just as heat-transfer fluids, however as possible cold-storage media also, due to this tunable behavior. Most of the current engineering applications however, consider W–EG to be a circulating fluid and not a storage medium. In a typical system, the mixture performs the cooling function, and the water, ice, and/or other PCM are responsible for the storage function [Yang, 2021], [Bello, 2025], [Yu, 2022]. Therefore, the experimental characterization of W–EG mixtures as storage media is still limited and is needed in a systematic manner. The summarized key studies relevant with the thermal energy storage application using PCM and the district cooling application are shown in Table 1.

Table 1: The literature reviewed is summarized and approaches/models used are presented

Study	Year	PCM	HTF	Model/Study Approach
[37]	2021	Review of organics, hydrates, molten salts, and metal alloys	Water and air	Reviewed PCM-based TES from a multiscale perspective using FEM, FVM, and AI-based optimization.
[45]	2020	Tetradecane and hexadecane mixture compared with ice	Brine with 50% ethylene glycol	Developed a 3D COMSOL model for packed-bed EPCM and ice storage, validated with DCS operating data.
[11]	2020	Paraffin emulsion and sodium acetate trihydrate	Water	Combined life-cycle assessment with system optimization to evaluate TES options in district energy systems.
[33]	2022	Eutectic paraffin wax and palmitic acid with TiO_2	Not mentioned	Synthesized nano-enhanced eutectic PCMs and tested morphology, thermal properties, and cycling stability.
[36]	2020	RT35 organic PCM	Water	Used a 3D enthalpy-porosity model in Fluent to analyses PCM melting in finned TES units.

The primary research gap that is addressed in this study is the absence of systematic experimental data for W–EG mixtures as cold, thermal storage media operating under the conditions of DCS. Previous DCS-TES research has focused on chilled-water storage, encapsulated PCM tanks and cascaded PCM packed-bed systems, but not in its

entirety on the storage medium, which is W–EG mixtures [Guillén-Lambea, 2021], [Shao, 2023], [Shao, 2020]. Most studies on PCM cooling have been conducted on either ice storage around 0 °C, where sub-zero heat transfer fluid temperatures are required or on organic PCMs that operate around 5-12 °C chilled water range, but may not meet the near zero or sub-zero heat storage requirement [Brancato, 2017], [Farah, 2019]. W–EG mixtures are used extensively as a brine or secondary refrigerant; however, they have not been extensively studied as a storage medium [Ukpe, 2022], [Bello, 2025]. It is also noted that other PCM research has been conducted to assess the properties of thermal conductivity, supercooling, phase stability, cycling reliability and the charging/discharging behavior for use in practical integration, but not usually in the same experimental setup [Jacob, 2022], [Yang, 2021], [Alva, 2017]. Specially, evidence of the effect of W–EG concentration on the phase-change temperature, cooling retention, storage density, supercooling tendency, charging time, discharge stability and energy consumption during full charging–discharging cycles is not found side-by-side. This dearth makes it hard to determine the best W–EG composition for practical cold TES for district cooling applications. The paper, therefore, experimentally explores the use of W–EG mixtures as potential candidates for the cold-storage media for district cooling TES. The study makes the following contributions:

1. In this study, water–ethylene glycol mixture is experimentally investigated for its use as the cold thermal energy storage medium for district cooling systems and its feasibility under practical operating conditions is analyzed.
2. It investigates the temperature change, cooling retention and operation stability of various W–EG mixture ratios under the same test conditions to study the charging and discharging performance.
3. It considers thermal performance along with energy consumption in complete operation cycles and determines the optimum mixture ratio for energy efficient and practical DCS cold-storage operation.

The materials and methods are described in Section 2, the experimental setup is presented in Section 3, the results and analysis will be discussed in Section 4 and the final findings and recommendations are given in Section 5.

2. Materials and Methods

2.1 Selection of Water–Ethylene Glycol as PCM

Ethylene glycol-water mixtures were chosen as the potential cold thermal energy storage medium due to their good thermophysical properties, subzero operation, and compatibility with district cooling systems [Gupta, 2018]. The latent heat of fusion and specific heat capacity of pure water is high, which makes it a good thermal storage material, however, its freezing point is 0 °C which is not suitable for it to be used for some direct cooling systems which operate below 0 °C because ice formation could block flow and destabilize the operation of the system. In order to overcome this limitation, ethylene glycol was added to lower the freezing temperature and enlarge the operating range of the TES system to be below 0 °C, while keeping the system low-temperature operational stability and maintaining compatibility with conventional refrigeration components. Water–ethylene glycol mixtures are also popular secondary refrigerants due to low costs, commercial availability, chemical stability, and less corrosivity than many salt-hydrate-based phase change materials. Six compositions of water ethylene glycol (EG) mixtures by mass, including pure water and 90/10, 80/20, 70/30, 60/40, and 50/50 water–EG, were chosen for experimental study to investigate the effect of ethylene glycol concentration on TES performance. Table 2 shows the approximate freezing points and the composition matrix. As the ethylene glycol concentration is increased, the freezing temperature drops progressively from 0 °C for pure water to about −36 °C for the 50/50 mixture as is shown in Table 1. The selected mixtures provide a wide operating range which allows for the investigation of charging and discharging behavior under district heating operating conditions.

Table 2: Water–ethylene glycol mixtures and their composition matrix and freezing points

Sample ID	Water (wt%)	Ethylene Glycol (wt%)	Approximate Freezing Point (°C)
S1	100	0	0
S2	90	10	−4
S3	80	20	−10
S4	70	30	−16
S5	60	40	−24
S6	50	50	−36

2.2 Sample Preparation

The experimental mixtures were prepared using industrial grade ethylene glycol (EG) that is purified > 99.5% and deionized water. For each composition, the order of preparation was as follows: about 25-30 L of each were prepared separately by using a calibrated digital balance (with uncertainty of ±0.01 kg) for obtaining the correct mass fractions. All the required quantity of water and ethylene glycol were measured separately and poured into a clean polyethylene mixing reservoir, and then the solution was thoroughly mixed by operating the mechanical mixing machine at low speed (about 200 rpm) for 10-15 min to eliminate concentration difference and to ensure complete homogenization of the solution before adding it to the TES reservoir tank. The mixed solution was then left to settle at room temperature (~25–28 °C) in the laboratory for at least one hour before experimental use. To ensure uniformity and repeatability in the experimental process, the reservoir tank, circulation piping, and centrifugal pump were completely emptied and flushed with deionized water after every charging/discharging cycle to prevent any cross-contamination between the different compositions. To guarantee equal operating conditions for the experimental analysis, the same preparation procedure was used for all six mixtures investigated.

2.3 Thermophysical Property Characterization

Thermophysical properties of the prepared water–ethylene glycol mixtures were determined as these will have a significant effect on charging behaviour, discharge stability, energy-storage density and pumping performance of the TES system. The properties studied were density, specific heat capacity, thermal conductivity, dynamic viscosity and freezing point. The density measurements were made with a calibrated vibrating-tube densitometer with an uncertainty of about ±0.5 kg/m^3, the specific heat capacity was determined based on the differential scanning calorimetry method, and the thermal conductivity measurements were made by the method of a transient hot-wire method with an uncertainty of about ±3%, and the dynamic viscosity was measured by the method of a controlled-strain rotational rheometer with a cone-and-plate geometry. The cooling curve was used to record the onset temperature of solidification for each of the mixture by applying the tangent intersection method to determine the freezing point. The calculated representative thermophysical properties of the investigated water–ethylene glycol mixtures are summarized in Table 3. The results showed that as the concentration of ethylene glycol increased, the density increased from about 998kg/m^3 to 1090kg/m^3; the viscosity increased from 1.0×10-3Pa·s to 5.5×10-3Pa·s; the specific heat capacity decreased from 4180 to 3100J/kg·K; and the thermal conductivity decreased from 0.60 to 0.33W/m·K. Furthermore, the freezing temperature continued to fall as the concentration of ethylene glycol increased, from 0 °C for pure water down to about 0 °C for a 50/50 mixture, showing that the mixture had better sub-zero operating ability as the concentration increased.

Table 3: Representative thermophysical properties of water–ethylene glycol mixtures

Property	Symbol	Representative Value	Unit
Density	ρ	1065	kg/m^3
Specific heat capacity	cp	3380	J/kg·K
Thermal conductivity	k	0.39	W/m·K
Dynamic viscosity	μ	3.4×10^{-3}	Pa·s
Freezing point	Tf	−36	°C

2.4 Governing equations

The thermal performance of the water–ethylene glycol (W–EG) thermal energy storage system was analyzed based on the experimental measurements of the temperature in the thermal reservoir, the load-side temperature, the time elapsed, and the accumulated electrical energy consumption. In order to reduce the data-reduction process and make the results of the experiments easier to interpret, the analysis was conducted in terms of comparative performance indicators and not the complete calculation of thermal efficiency. The temperature of the reservoir was taken as uniform and the heat loss from the insulated tank to the surroundings was neglected for the duration of the experiments. To determine the temperature drop of the PCM mixture during charging, the temperature difference between the initial temperature of the reservoir and the final temperature of the reservoir during charging was calculated as expressed in Eq. (1) [Wang, 2026]. The average charging rate was then calculated by dividing the total temperature reduction with the total charging time as mentioned in Eq (2). Energy measured by the cumulative meter reading during charging was calculated by subtracting the initial cumulative energy meter reading from the final cumulative energy meter reading as per Eq. (3) [Karimi, 2021]. The energy requirement of each mixture was determined by dividing energy consumption by the amount of temperature reduction, from Eq. (4) [Pourebrahim, 2026].

$$\Delta T = T_i - T_f \tag{1}$$

$$R_c = \frac{\Delta T}{t_c} \tag{2}$$

$$E_c = E_f - E_i \tag{3}$$

$$E_{\Delta T} = \frac{E_c}{\Delta T} \tag{4}$$

Where T_i is the initial reservoir temperature, T_f is the final reservoir temperature, ΔT is the total temperature reduction, R_c and t_c is the average charging rate and total charging time respectively. Also, E_c, E_i and E_f is the net charging energy consumption, initial energy-meter reading and the final energy-meter reading respectively. Although, $E_{\Delta T}$ is the electrical energy required for each degree Celsius reduction in reservoir temperature. The cooling delivery performance was determined from the discharge duration and load side temperature response during discharging. The discharge time was determined by subtracting the initial and end discharge times from the last two readings, and applying Eq. (5). The load-side cooling condition was deemed to be effective if the load temperature was kept in the experimental target range, which is shown in Eq. (6). Discharging energy index was calculated for the mixtures for which the discharging energy readings were available, using Eq. (7) [Martínez-Ángeles, 2025].

$$t_d = t_f - t_i \tag{5}$$

$$13^\circ C \leq T_L \leq 15^\circ C \tag{6}$$

$$I_d = \frac{E_d}{t_d} \tag{7}$$

where $t_d$is the discharge duration, $t_i$is the initial discharge time, $t_f$is the final recorded discharge time, $T_L$is the load-side temperature, $I_d$is the discharging energy index, and $E_d$is the cumulative electrical energy consumed during discharge.

2.5 Experimental Uncertainty

This experimental uncertainty analysis was used to assess the reliability of the measured and derived thermal-performance parameters. The digital energy meter and flow meter have uncertainties of around ±1% and ±2% respectively, and the calibrated thermocouples used for measuring the reservoir and load temperatures had an uncertainty around ±0.5 °C. The total uncertainty of discharge energy and round-trip efficiency was about ±5%, similar to other laboratory-scale thermal energy storage experiments found in the literature.

3. Experimental Analysis

3.1. Experimental setup

The experimental setup was a laboratory-scale thermal energy storage rig connected to a vapour-compression refrigeration system, to examine the charging and discharging characteristics of the water–ethylene glycol mixture for the district cooling operation. This was an integrated system consisting of a thermally insulated TES reservoir tank, a vapor-compression refrigeration loop, and a secondary heat-transfer-fluid circulation system linked to prototype building enclosures to simulate the buildings' cooling load. The refrigeration section comprised a hermetic reciprocating compressor, air-cooled condenser along with thermostatic expansion valve and a submerged evaporator coil in the TES reservoir, the secondary loop comprised centrifugal circulation pump, solenoid valves, gate valves, inline flow meters, and load-side heat exchangers. The evaporator was submerged into the storage medium during charging to absorb heat from the storage medium and was cooled below 0 °C during discharging, the cooled heat transfer fluid was circulated through the secondary loop to transfer the cooling energy stored in the storage medium to the prototype building enclosures. The effective storage capacity of the TES reservoir was around 25 L and the reservoir was externally insulated to reduce heat loss to the surrounding environment. The schematic arrangement of the experimental system is shown in Fig. 1 and the front view of the experimental system is shown in Fig. 2.

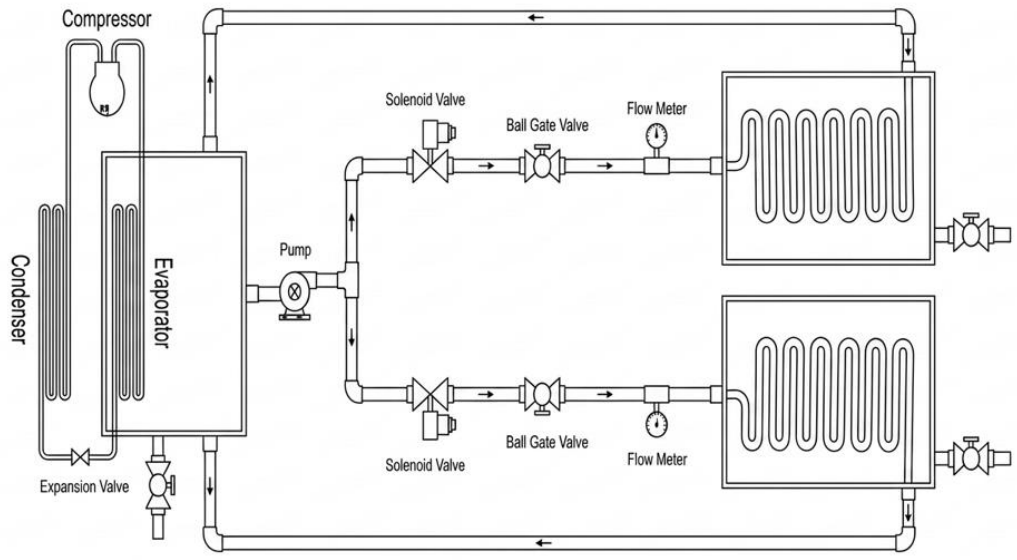

Fig. 1. Schematic of the experimental thermal energy storage test rig used in this study

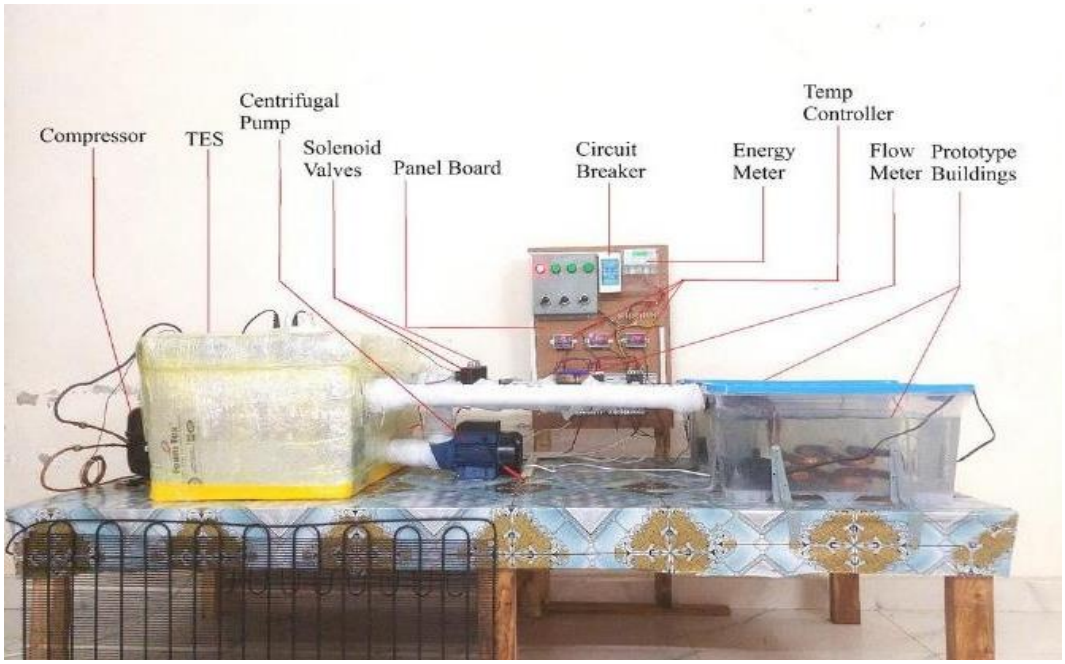

Fig. 2. Front view of the constructed experimental setup

The measuring instruments and the uncertainties associated with them are summarized in Table 4. Reservoir and load side temperatures were recorded using calibrated T-type thermocouples (uncertainty ± 0.1 °C) while the cumulative electrical energy consumption was measured by a Class 1 digital energy meter (uncertainty ± 1.0%). The volumetric flow rate was measured with the use of inline turbine flow meters, with an uncertainty of ±1.5%, for the HTF. The data of all the sensors were acquired by a USB based data acquisition system at 1 Hz sampling frequency and all the instruments were calibrated before the experiments.

Table 4: Instrument specifications and measurement uncertainties for the experimental test

Quantity	Instrument / model	Range	Uncertainty
Reservoir or load temperature	T-type thermocouple, calibrated	−40 to +60 °C	±0.1 °C
Cumulative electrical energy	Class-1 single-phase energy meter	0–10 kWh	±1.0%
Pump volumetric flow rate	Inline turbine flow meter	0.5–3.0 L/min	±1.5%
Reservoir or load tank volume	Calibrated graduated mark	0–30 L	±0.2 L
Sample composition (mass)	Digital balance	0–50 kg	±0.01 kg
Density	Vibrating-tube densitometer	0.8–1.2 g/cm³	±0.5 kg/m³
Specific heat	DSC (5 °C/min)	−50 to +30 °C	±2.0%
Thermal conductivity	Transient hot-wire apparatus	0.1–1.0 W/(m·K)	±3.0%

3.2 Charging procedure

The charging process was carried out by the vapor-compression refrigeration loop as shown in Fig. 1. Prior to each charging experiment the reservoir tank of the TES was emptied, scrubbed and refilled with a new charge of the desired water–ethylene glycol composition. The reservoir was filled and left to stabilize at the laboratory ambient temperature (24–26 °C) for at least 30 min, for uniform initial conditions. The refrigeration system was then switched on and the digital temperature controller was set with the charging setpoint about 2 °C lower than the freezing temperature of the mixture which was to be frozen. While charging, heat was removed directly from the TES

reservoir by the submerged evaporator, lowering the mixture temperature gradually towards the desired sub-zero temperature. Data-acquisition system measured the reservoir temperature, ambient temperature, elapsed time and cumulative electrical energy consumption data at a sampling rate of 1 Hz. When the temperature of the reservoir hit the setpoint for charging, and stayed within 0.5 °C of that setpoint for a minimum period of 10 minutes after switching on the charging heater, the charging process was terminated, and the refrigeration compressor was then turned off, letting the TES reservoir stabilize thermally before the discharge cycle was begun.

3.3 Discharging procedure

The discharging process was performed with secondary HTF circulation loop presented in Fig. 1. After charging, the refrigeration compressor was turned off and the recirculation valves between the TES reservoir and the building branches were opened. The cooled water–ethylene glycol mixture was then pumped through the inline turbine flow meters and into the load-side coil heat exchangers submerged in the prototype building enclosures, which resulted in the transfer of the stored cooling energy from the TES reservoir to the simulated cooling load. The prototype building enclosure was pre-conditioned to a typical return temperature of the District Heating (DH) return water, which was about 22–25 °C, before it was discharged. The reservoir temperature, load side temperature and duration of discharge were monitored continuously. The circulation pump was operated in a temperature-controlled feedback mode, with the pump briefly shutting down whenever the temperature at the load side reached around 13 °C and then re-enabling after a set dwell time to reconnect the load to the rest of the cold inventory in the TES reservoir. The discharge cycle was ended when the temperature of the load side was not able to be lowered to the desired chilled water temperature in one circulation cycle.

3.4 Test matrix and repeatability

A series of six different water–ethylene glycol mass ratios (100/0, 90/10, 80/20, 70/30, 60/40, and 50/50) were experimentally studied. Each composition was charged and discharged one time to the same extent with the same operating conditions. Repeatability was assessed by repeating each experiment three times after re-batching the storage medium and the differences between the repeated experiments for the main discharge variables were less than 3.5%. In Section 4 the results shown are the mean values of the repeated experiments. Besides, a baseline test was performed on a sensible-cooling mode on the experimental rig with pure water to confirm that the experimental rig is consistent with the conventional chilled-water storage mode reported in literature without sub-zero charging.

3.5 Data processing

The raw experimental data from the temperature, energy and flow channels were synchronized with the common time stamp of the data acquisition system before analysis. The drift introduced by the self-heating effects in the thermocouples was corrected with the calibration of the thermocouples provided by the manufacturer, and high frequency noise in the temperature signals was removed by five-point moving-average filtering. The sum of the charging and discharging energies were computed from the governing equations given in Section 2.4, and then the round-trip efficiency and the volumetric energy-storage density were obtained from the processed results. The Gaussian uncertainty-propagation method was used to propagate experimental uncertainty to values derived from the measurements and the instrument uncertainties listed in Table 2.

4. Results and Discussion

In this section, the charging and discharging experimental results of the studied water-ethylene glycol mixtures for thermal energy storage in a district cooling system are presented. The discussion is organized in three steps: individual graph interpretation, comparative charging analysis and comparative discharging analysis. The information used is only the measured temperature, time and cumulative electrical-energy data found in the experimental record. The mass, latent heat and load-side flow-rate for PCM are not available for all cases, and full round-trip thermal efficiency is not reported, but instead charging-energy index, average charging rate, discharge duration and discharge energy index are used as comparative performance metrics.

4.1 Charging behaviour of the investigated mixtures

The charging process is the heat being extracted from the storage medium by the vapor-compression refrigeration unit [Yan, 2019]. For this data set, there are no charging data for 100% water, 80% water and 20% ethylene glycol, and 70% water + 30% ethylene glycol. Comparisons are based on temperature reduction in the reservoir, the overall charging time, total electrical energy usage, and average charging rate.

4.1.1 Charging behaviour of 100% water

In 100% water case, the temperature of the reservoir drops from 19.1 °C to 2.0 °C in 14.51 min and the cumulative electrical energy consumption increases from 0.00 kWh to 0.64 kWh in the same time. This result indicates that the charging time for pure water was the shortest and the electrical energy was the least for the available charging tests. At the end of the test, however, the temperature was still above 0 °C, so the test did not demonstrate sub-zero storage behaviour. The charging profile which corresponds to this is displayed in Fig. 3.

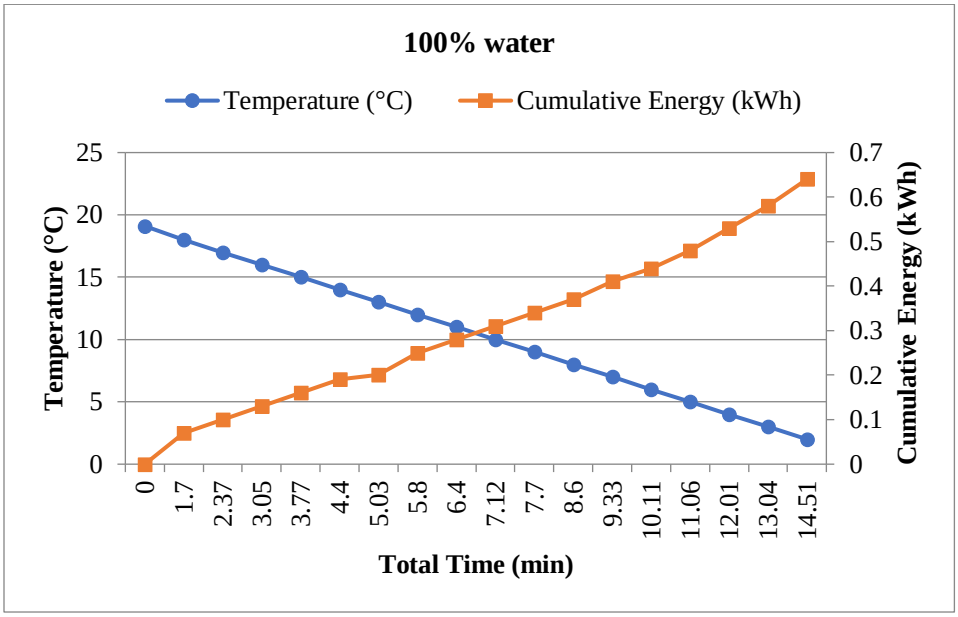

Fig. 3. Charging profile of the 100% water

4.1.2 Charging Behaviour of Ethylene Glycol Mixtures

The two-ethylene glycol charging mixtures consisted of 80% water and 20% ethylene glycol; and 70% water and 30% ethylene glycol. The two mixtures cooled below freezing and pure water above 0 °C. The 80% water and 20% ethylene glycol mixture cooled from 19.7 °C to -6.0 °C in 26.84 min and consumed 1.13 kWh. This indicates that low-temperature charging range was enhanced by using ethylene glycol, while the charging time and charging energy were increased. The charging profile for the 80% water / 20% ethylene glycol mixture is shown in Fig. 4.

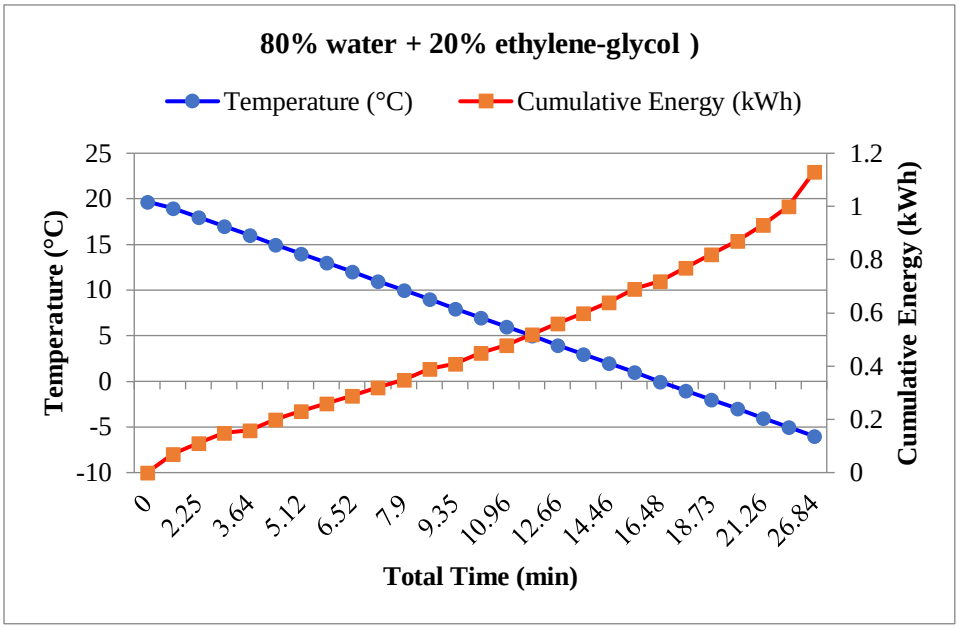

Fig. 4. Charging profile of the 80% water and 20% ethylene glycol mixture

The 70% water and 30% ethylene glycol solution had the deepest charging of all the charging tests used. The temperature in the reservoir dropped from 27.6 °C to -9.0 °C in 34.90 min and the cumulative electrical energy was 1.54 kWh. This meant that the subzero operating range of the storage medium was extended with the increase of ethylene glycol concentration. But the deeper cooling was obtained in the longest charging time and highest energy consumption. The charging behaviour of the 70% water and 30% ethylene glycol mixture is shown in Fig. 5.

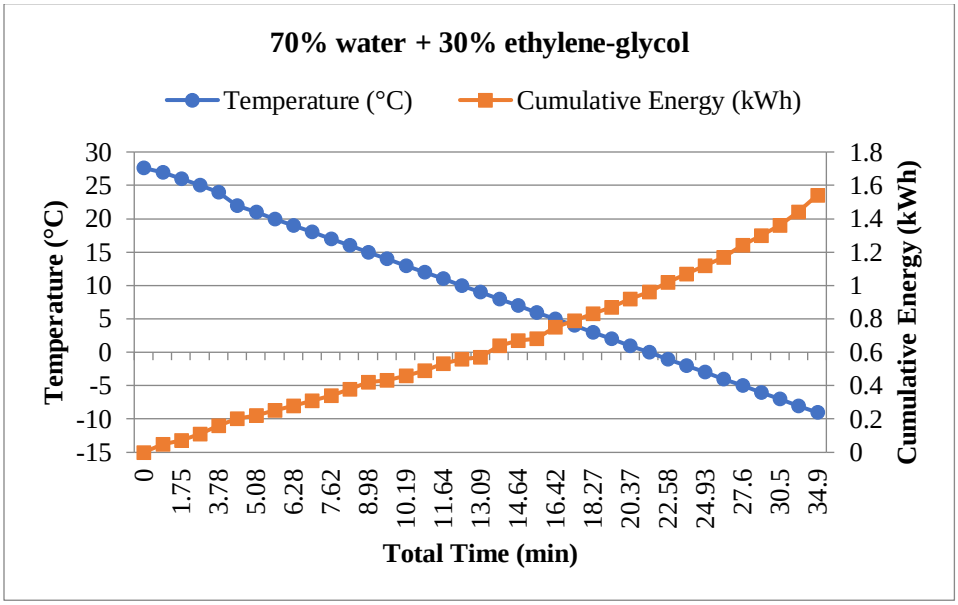

Fig. 5. Charging profile of the 70% water and 30% ethylene glycol mixture

4.1.3 Comparative Charging Performance

A summary of the charging performance of the mixtures tested is given in Table 5. The table shows comparative data for the initial temperature, final temperature, temperature reduction, total charging time, cumulative electrical energy, and average charging rate. Through this comparison, it is possible to determine the impact of ethylene glycol concentration on charging depth and energy requirements.

Table 5: Comparative charging performance of the tested mixtures

PCM mixture	Initial temp. (°C)	Final temp. (°C)	Temp. reduction (°C)	Total charging time (min)	Final cumulative energy (kWh)	Average charging rate (°C/min)
100% Water	19.1	2.0	17.1	14.51	0.64	1.18
80% Water with 20% EG	19.7	-6.0	25.7	26.84	1.13	0.96
70% Water with 30% EG	27.6	-9.0	36.6	34.90	1.54	1.05

Table indicates that the mixture of 70% water and 30% ethylene glycol had the greatest temperature difference between the initial and final charging temperatures recorded. The 100% water case took the shortest charging time and energy but was not able to achieve sub-zero temperatures. The 80/20 water-to-ethylene glycol solution had an intermediate effect, reaching sub-zero temperature using less energy and charging time than the 70/30 solution. A charging-energy performance index was determined to compare the electrical energy needed to reduce the temperature by a degree Celsius. The results of calculations are given in Table 6.

Table 6: Charging-energy performance index

PCM mixture	Temperature reduction (°C)	Energy consumed (kWh)	Energy per °C reduction (kWh/°C)
100% Water	17.1	0.64	0.037
80% Water and 20% EG	25.7	1.13	0.044
70% Water and 30% EG	36.6	1.54	0.042

Table shows that the case with the 100% water use had the lowest energy demand per degree of temperature drop. This result must be taken with a pinch of salt though, as pure water was not brought down to sub-freezing temperatures. The 70/30 mixture of ethylene glycol had a slightly lower energy-per-degree value than the 80/20 mixture, but a lower final temperature. Hence, the 70/30 mixture showed a better sub-zero charging capability, and the 80/20 mixture showed a moderate sub-zero charging requirement.

4.2 Discharging Behaviour of the Investigated Mixtures

The discharging behaviour was assessed from the temperature of the reservoir, the discharge side temperature, the time of the last discharge and the total discharge energy [Yang, 2023]. The goal of the discharging analysis was to assess the cooling capacity of each mixture on the load side and to see how long the load temperature could be kept within the experimental target range for the load side (13–15 °C).

4.2.1 Charging behaviour of 100% water

The study examined the discharge behaviors of 100% water. Here, the reservoir temperature was 2.0 °C at start of test and the initial load temperature was 18.6 °C for the 100% water discharge test. By the early stages of the discharge, the load temperature was 13.0 °C and the reservoir temperature at the end of the recorded data was 8.2 °C. This means that, during discharge, the pure water could cool the water flow by undergoing sensible cooling. For this case only temperature response and recorded time behaviour was considered, but no cumulative discharge energy was available. The discharge profile for the case is displayed in Fig. 6.

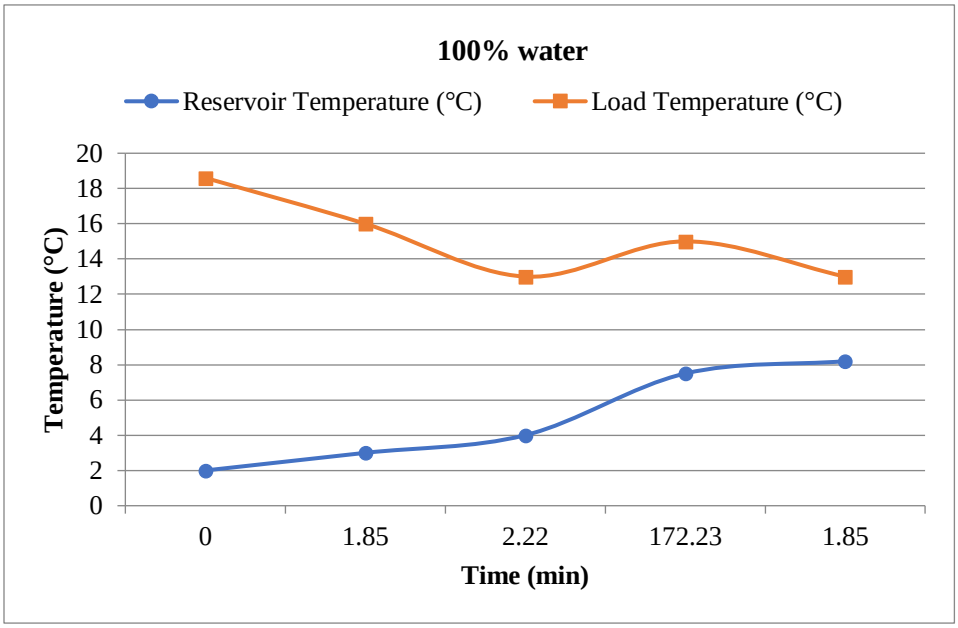

Fig. 6. Discharging profile of the 100% water case showing reservoir and load-side temperatures

4.2.2 Discharging Behaviour of Intermediate Ethylene Glycol Mixtures

The intermediate ethylene glycol mixtures were composed of 90% water + 10% ethylene glycol, 80% water + 20% ethylene glycol, and 70% water + 30% ethylene glycol. The observed discharge times for these mixtures were different although the temperature drop on the load side was the same for all of them (13.0 °C). The 90% water/ 10% ethylene glycol mixture has been discharged with a reservoir temperature of -2.0 °C and an initial load temperature of 22.3 °C. The longest discharge time was 191.23 min recorded, and the recorded discharge data are the longest periods. The final load temp- 13.0 °C. This indicates good cooling retention and stable load-side temperature behaviour of the 90% water/10% ethylene glycol solution. The discharging profile of the 90% water and 10% ethylene glycol mixture is shown in Fig. 7.

.

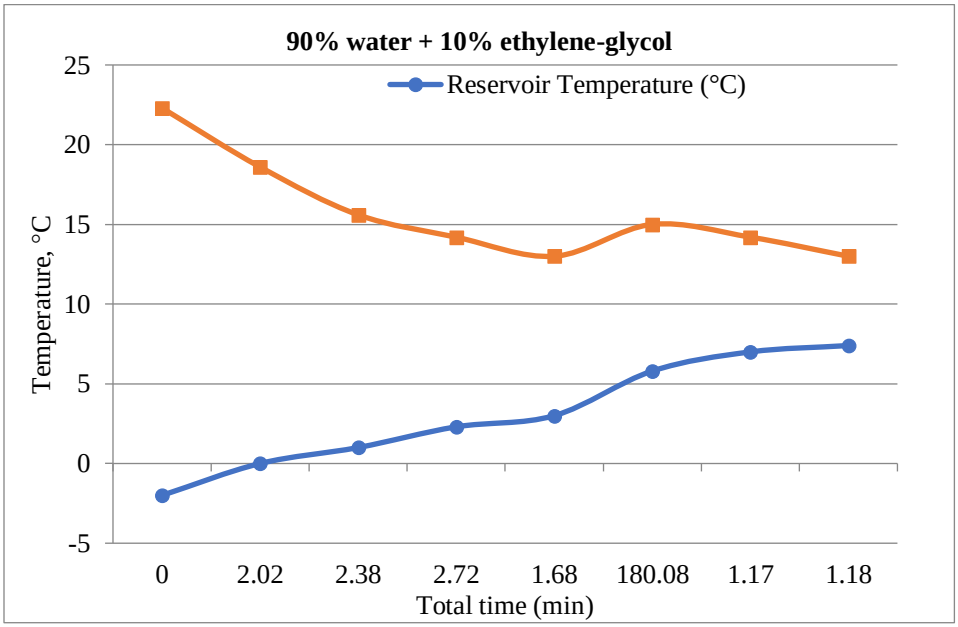

Fig. 7. Discharging profile of the 90% water and 10% ethylene glycol mixture

The mixture of 80% water and 20% ethylene glycol was at a water reservoir temperature of -5.0 °C and a load temperature of 17.4 °C. The final discharge time was 175.60 minutes, and the final load temperature was 13.0 ° C.

This means that the mixture was able to provide effective cooling well after the end of the run and within the set cooling range. Fig. 8 shows the variation of the temperature of reservoir and load in the case of a 20% ethylene glycol and 80% water solution.

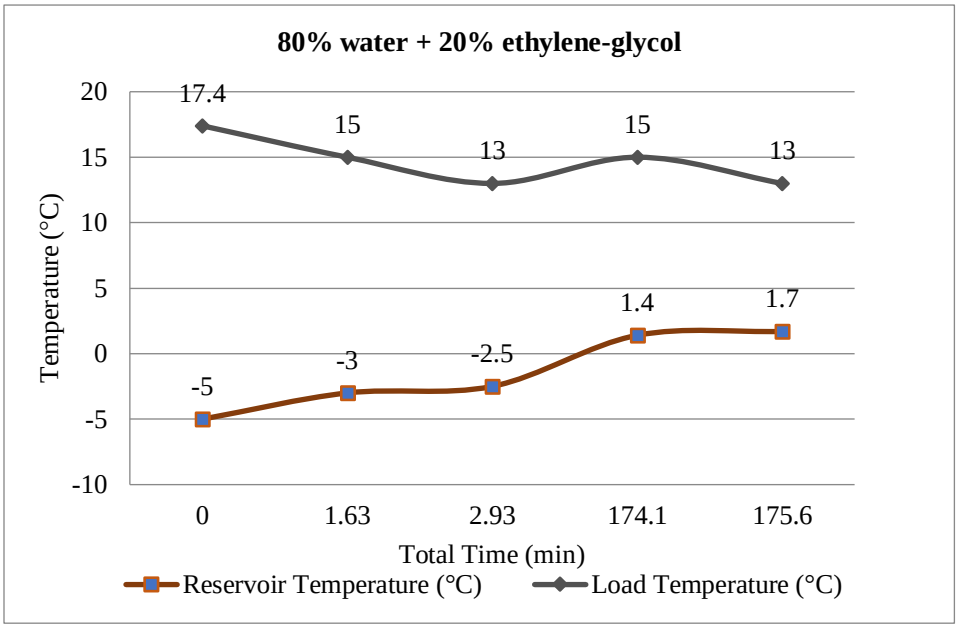

Fig. 8. Discharging profile of the 80% water and 20% ethylene glycol mixture

The 70 % water, 30 % ethylene glycol solution was discharged with the water temperature of the reservoir being -9.5 °C and the temperature of the initial load being 24.8 °C. This mixture started with a lower reservoir temperature, but the final time recorded was 88.96 min. The final load temperature was 13.0 °C. This suggests that the initial reservoir temperature was not always higher when the discharge period was longer, as was the case in the data recorded. The schematic of the discharging behaviour of the 70/30 mix of water and ethylene glycol is shown in Fig. 9.

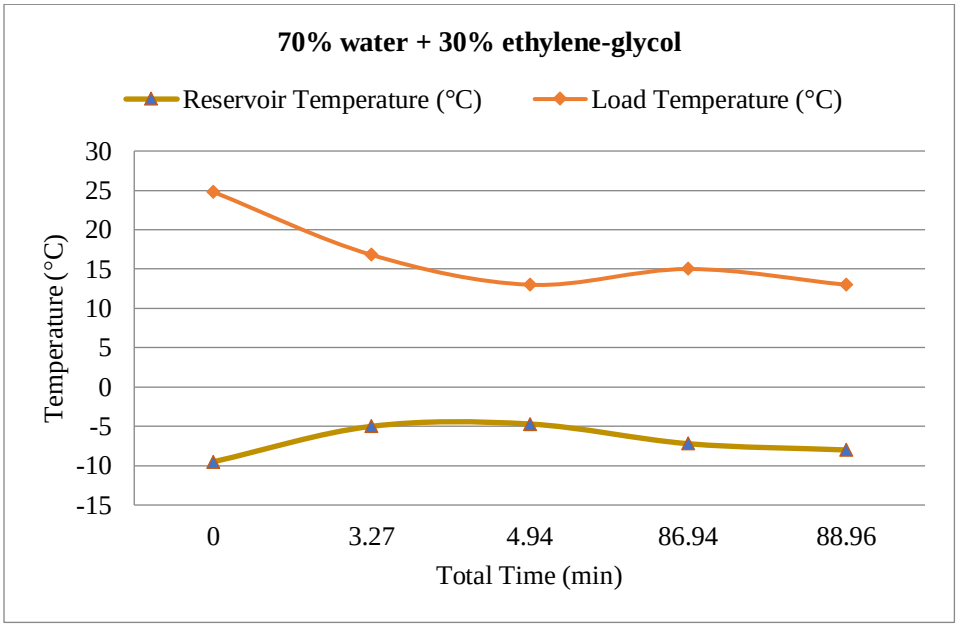

Fig. 9. Discharging profile of the 70% water and 30% ethylene glycol mixture

4.2.3 Discharging Behaviour of High Ethylene Glycol Mixtures

The discharging behaviour of high ethylene glycol mixtures is explained. The ethylene glycol mixtures with the highest concentration were 50% water and 50% ethylene glycol and 60% water with 40% ethylene glycol. The discharge time in both of these mixtures was greater than 180 min and the cumulative discharge energy was known for both. The initial temperature of the water (22.0 °C) and ethylene glycol (22.0 °C) mixture was 50%, and the temperature of the reservoir was 22.0 °C at the start of discharge. Within early stage of discharge, the load temperature was 13.0 °C. Following reactivation of the pump, the system continued to run until the final discharge time was 182.03 min. The total discharge energy is 0.04 kWh. This result demonstrates that the 50% water/50% ethylene glycol mixture has long duration cooling, but has slightly higher discharge energy consumption than the 60% water/40% ethylene glycol mixture. The results for a 50% water/50% ethylene glycol mixture are shown in Fig. 10.

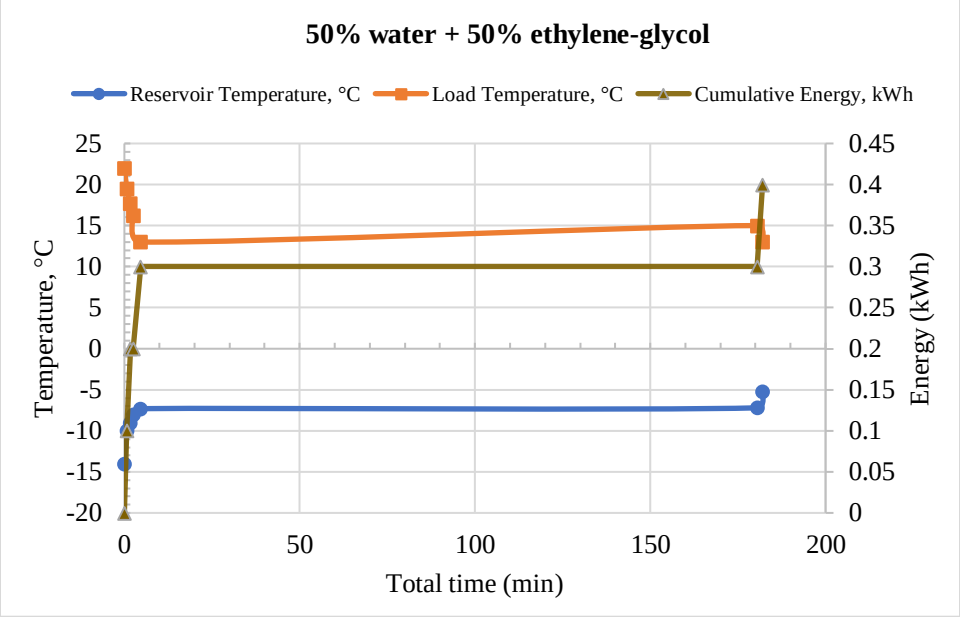

Fig. 10. Discharging profile of the 50% water and 50% ethylene glycol mixture

The 60% water and 40% ethylene glycol mixture started discharge with a reservoir temperature of -10.0 °C and an initial load temperature of 24.5 °C. The final discharge time was 180.68 min and the end of the discharge energy was 0.03 kWh. The mixture kept the load side temperature within 13-15℃ operating range, which was the reason for stable cooling delivery. The discharge characteristics of the 60% water, 40% ethylene glycol solution are given in Fig. 11.

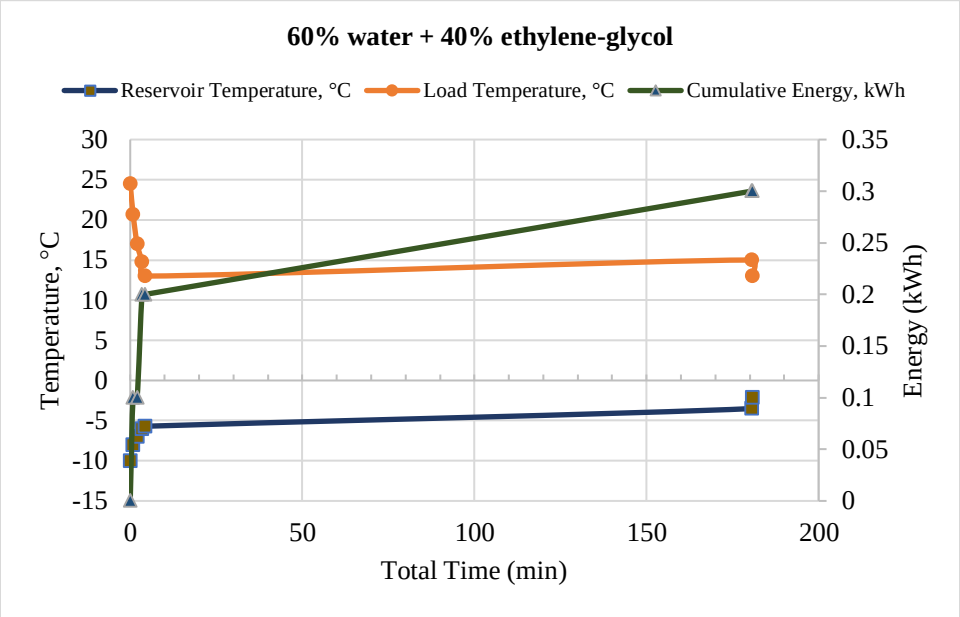

Fig. 11. Discharging profile of the 60% water and 40% ethylene glycol mixture

4.2.4 Comparative Discharging Performance

The comparative discharging performance of all the tested mixtures is summarized in Table 7. This table details the initial and final reservoir temperature, initial and final load temperature, final recorded time and, if available, the cumulative discharge energy.

Table 7: Comparative discharging performance of the tested mixtures

PCM mixture	Initial reservoir temp. (°C)	Final reservoir temp. (°C)	Initial load temp. (°C)	Final load temp. (°C)	Final recorded time (min)	Final cumulative energy (kWh)
100% Water	2.0	8.2	18.6	13.0	N/A	N/A
90% Water with 10% EG	-2.0	7.4	22.3	13.0	191.23	N/A
80% Water with 20% EG	-5.0	1.7	17.4	13.0	175.60	N/A
70% Water with 30% EG	-9.5	-8.0	24.8	13.0	88.96	N/A
60% Water with 40% EG	-10.0	-2.1	24.5	13.0	180.68	0.03
50% Water with 50% EG	-14.0	-5.2	22.0	13.0	182.03	0.04

From Table 7, it can be seen that the 90% water and 10% ethylene glycol mixture gave the longest discharge time and the 50% water and 50% ethylene glycol mixture gave the second longest discharge time while the 60% water and 40% ethylene glycol mixture gave the third longest discharge time. The 70/30 water/ethylene glycol solution began at a lower reservoir temperature, but has a shorter recorded discharge time. This means that the only initial reservoir temperature cannot be used to assess the discharge performance. Other parameters of interest are load-side temperature stability and the total discharge time for district cooling applications. The discharge-energy index for the mixtures for which energy data were available is compared with one another in Table 8. Only mixtures of 60% water and 40% ethylene glycol and 50% water and 50% ethylene glycol were reported in this index because cumulative discharge energy figures are available for these cases only.

Table 8: Discharging-energy index for mixtures with available discharge-energy data

PCM mixture	Final recorded time (min)	Final cumulative discharge energy (kWh)	Energy index (kWh/min)
60% Water + 40% EG	180.68	0.03	0.000166
50% Water + 50% EG	182.03	0.04	0.000220

This table indicates that the discharge-energy index of the 60% water and 40% ethylene glycol mixture was lower than the 50% water and 50% ethylene glycol mixture. This was based on the assumption that, in the range of discharge-energy records available, the 60% water and 40% ethylene glycol mixture needed less electrical energy per minute to record the discharge operation. This index should not be treated as full discharging efficiency as it does not take into consideration the useful thermal energy output.

4.4 Discussion

The charging results showed that the addition of ethylene glycol enhanced the subzero charging ability of the storage medium, but it resulted in longer charging time and energy consumption. The temperature of the water in the reservoir went down by 2.0 °C, which is about 17.1 °C, after 14.51 min in pure water, and the end cumulative energy consumption was 0.64 kWh. This was the shortest charging time and energy consumption of the available charging tests and pure water did not get to sub-zero temperature. The 80% water and 20% ethylene glycol mixture, on the other hand, when cooling from 19.7 °C to -6.0 °C, had a greater temperature drop of 25.7 °C and required 1.13 kWh of energy to achieve this reduction in 26.84 min. The deepest charging was observed in the 70% water + 30% ethylene glycol mixture which reduced the temperature from 27.6 °C to -9.0 °C (a decrease of 36.6 °C in 34.90 min with an energy consumption of 1.54 kWh). Hence, the 70/30 mixture has the lowest final temperature and the greatest temperature difference but it has the longest charging time and the highest electrical energy input. The 80/20 mixture produced an intermediate result which was able to be charged to sub-zero charging with less energy and charging time than the 70/30 mixture. In the discharging results, it is not only the lowest initial reservoir temperature that is important as a criterion for the longest cooling duration. The 70/30 mixture had a relatively low temperature in the reservoir of -9.5 °C, and brought the load temperature down from 24.8 °C to 13.0 °C, but it was only able to discharge for 88.96 min. The 90% water + 10% ethylene glycol mixture, on the other hand, was initiated at a higher temperature in the reservoir (22.3 °C), but maintained the longest recorded discharge time of 191.23 min and lowered the load temperature from 22.3 °C to 13.0 °C. The mixture of 80/20 also exhibited a relatively constant discharge temperature beginning at -5.0 °C reservoir temperature and ending with a discharge time of 175.60 min with a load temperature that dropped from 17.4 °C to 13.0 °C. The high-glycol mixtures also had long discharge times: the 60/40 mixture discharged for 180.68 min to a final cumulative discharge energy of 0.03 kWh, and the 50/50 mixture discharged for 182.03 min to a final cumulative discharge energy of 0.04 kWh. The most appropriate mixture from these data is the 70/30 mixture for deeper charging in sub-zero temperatures, the 90/10 mixture for longer discharge times and the 80/20 mixture can be considered the best compromise in terms of overall performance and was able to reach sub-zero temperatures with not too high energy consumption and then assure a longer discharge time. Since full charging data were not available for the 60/40 and 50/50 mixtures, it is not advisable to rank them in this context without the thorough analysis of charging–discharging data provided by complete charging–discharging tests.

5. Conclusions

This study was a practical experimental test to assess the water–ethylene glycol mixture as a potential candidate cold thermal energy storage medium for district cooling applications, where temperature of the reservoirs, load-side temperature, elapsed time and cumulative electrical energy consumption were measured. The charging results indicated that adding ethylene glycol to the storage medium enhances the sub-zero operating capability: Pure water was cooled to -6.0 °C using charging energy of 1.13 kWh and it was cooled to -9.0 °C using charging energy of 1.54 kWh for the storage medium of 80/20 (water/ethylene glycol) and 70/30 (water/ethylene glycol) respectively. The 70/30 mixture led to the most cooling, while the 80/20 mixture had a more even response in sub-zero charging, charging time and energy usage. In discharging, the 90/10 (90% water with 10% ethylene glycol) mixture resulted in a discharging duration of 191.23 min, the 60/40 mixture in discharging duration of 180.68 min

and the 50/50 mixture in discharging duration of 182.03 min with a cumulative discharging energy of 0.03 kWh and 0.04 kWh, respectively, which are the longest discharging duration recorded. The results showed that the minimum reservoir temperature is not the only criterion to use in mixture selection for district cooling thermal storage, but the energy required for charging the reservoir, the time of discharge and the stability of the temperature at the load side must also be taken into account. This study has a few limitations, like full mass-flow-rate data, latent heat, inlet–outlet temperature difference, and useful cooling-energy data were not available for all mixtures, so full charging efficiency, discharging efficiency and round-trip efficiency were not reported. The 80/20 mixture can be used as an intermediate practical thermal energy storage solution when compared with the 70/30 and 90/10 mixtures, as, based on the available experimental results, the 90/10 is more suitable for deeper subzero charging while the 70/30 is suitable for deeper subzero charging. Future research should involve complete flow-rate measurement, helpful calculation of cooling-energy, repeated thermal cycling test, long-term stability test, corrosion assessment and scale-up analysis in real district-cooling operating conditions.

Acknowledgements: The authors would like to express their gratitude to the Department of Mechanical Engineering at Dhaka University of Engineering & Technology (DUET) for academic support and facilities to perform this research work in Gazipur, Bangladesh. The authors also thank everybody who gave technical assistance and constructive suggestions in the course of experimental work and in writing of the manuscript.

Competing Interest: The authors declare that they have no known competing financial interests or personal relationships that could have appeared to influence the work reported in this paper.

Authorship Contribution

Sharmin Akter was involved in conceptualization, methodology, experimental investigation, data collection, data visualization, analysis and original draft preparation of the manuscript. Md. Anowar Hossain supervised, methodological assistance, technical guidance, validation and reviewed and edited the manuscript. Hasan M. M. Afroz has contributed supervision, material support, validation, critical review and manuscript support and editing. The authors have seen and approved the final draft of the manuscript.

References

[1] Bandyopadhyay B. and Banerjee M., (2022) Decarbonization of cooling of buildings, *Solar Compass*, vol. 2, p. 100025, Aug. 2022, doi: 10.1016/j.solcom.2022.100025.

[2] Waite M., Cohen E., Torbey H., Piccirilli M., Tian Y., and Modi V., (2017) Global trends in urban electricity demands for cooling and heating, *Energy*, vol. 127, pp. 786–802, May 2017, doi: 10.1016/j.energy.2017.03.095.

[3] Duan Z., Omrany H., and Zuo J., (2025) Impact of climate change on energy performance and energy conservation measures effectiveness in Australian office buildings, *Energy*, vol. 319, p. 134956, Mar. 2025, doi: 10.1016/j.energy.2025.134956.

[4] Mohamed A., Lorestani N., and Shabani F., (2025) Impact of urbanization on land surface temperature: A global perspective, *Current Research in Environmental Sustainability*, vol. 10, p. 100315, 2025, doi: 10.1016/j.crsust.2025.100315.

[5] Liang Z. *et al.*, (2016) Heat wave, electricity rationing, and trade-offs between environmental gains and economic losses: The example of Shanghai, *Applied Energy*, vol. 184, pp. 951–959, Dec. 2016, doi: 10.1016/j.apenergy.2016.06.045.

[6] Al-Nini A., Ya H. H., Al-Mahbashi N., and Hussin H., (2023) A Review on Green Cooling: Exploring the Benefits of Sustainable Energy-Powered District Cooling with Thermal Energy Storage, *Sustainability*, vol. 15, no. 6, p. 5433, Mar. 2023, doi: 10.3390/su15065433.

[7] Oró E., Gil A., Miró L., Peiró G., Álvarez S., and Cabeza L. F., (2012) Thermal Energy Storage Implementation Using Phase Change Materials for Solar Cooling and Refrigeration Applications, *Energy Procedia*, vol. 30, pp. 947–956, 2012, doi: 10.1016/j.egypro.2012.11.107.

[8] Liu M., Saman W., and Bruno F., (2012) Review on storage materials and thermal performance enhancement techniques for high temperature phase change thermal storage systems, *Renewable and Sustainable Energy Reviews*, vol. 16, no. 4, pp. 2118–2132, May 2012, doi: 10.1016/j.rser.2012.01.020.

[9] Gao Z., Boudreaux P., Shabtay Y., Carmeli-Shabtay N., Nawaz K., and Vineyard E. A., (2026) Novel thermal energy storage component: Development, performance, and phase transition diagnosis, *Energy Conversion and Management*, vol. 348, p. 120682, Jan. 2026, doi: 10.1016/j.enconman.2025.120682.

[10] Tang H., Yu J., Geng Y., Liu X., and Lin B., (2023) Optimization of operational strategy for ice thermal energy storage in a district cooling system based on model predictive control, *Journal of Energy Storage*, vol. 62, p. 106872, Jun. 2023, doi: 10.1016/j.est.2023.106872.

[11] Guillén-Lambea S., Carvalho M., Delgado M., and Lazaro A., (2021) Sustainable enhancement of district heating and cooling configurations by combining thermal energy storage and life cycle assessment, *Clean Techn Environ Policy*, vol. 23, no. 3, pp. 857–867, Apr. 2021, doi: 10.1007/s10098-020-01941-9.
[12] McKenna P., Turner W. J. N., and Finn D. P., (2021) Thermal energy storage using phase change material: Analysis of partial tank charging and discharging on system performance in a building cooling application, *Applied Thermal Engineering*, vol. 198, p. 117437, Nov. 2021, doi: 10.1016/j.applthermaleng.2021.117437.
[13] Mao S., Liu Y., Wu X., Zhang L., Chen J., and Zhou T., (2025) Thermal energy storage performance, application and challenge of phase change materials: a review, *Energy Storage and Saving*, vol. 4, no. 3, pp. 300–322, Sep. 2025, doi: 10.1016/j.enss.2025.03.001.
[14] Dzhonova-Atanasova D., Georgiev A., Nakov S., Panyovska S., Petrova T., and Maiti S., (2022) Compact Thermal Storage with Phase Change Material for Low-Temperature Waste Heat Recovery—Advances and Perspectives, *Energies*, vol. 15, no. 21, p. 8269, Nov. 2022, doi: 10.3390/en15218269.
[15] Heier J., Bales C., and Martin V., (2015) Combining thermal energy storage with buildings – a review, *Renewable and Sustainable Energy Reviews*, vol. 42, pp. 1305–1325, Feb. 2015, doi: 10.1016/j.rser.2014.11.031.
[16] Shao Y. L., Soh K. Y., Islam M. R., and Chua K. J., (2023) Thermal, exergy and economic analysis of a cascaded packed-bed tank with multiple phase change materials for district cooling system, *Energy*, vol. 268, p. 126746, Apr. 2023, doi: 10.1016/j.energy.2023.126746.
[17] Vielma C. A., Majó M., Calderón A., Svobodova-Sedlackova A., Fernández A. I., and Barreneche C., (2026) Life cycle assessment of a conventional thermal energy storage system versus an alternative steel slag-based system for concentrating solar power plants, *Journal of Energy Storage*, vol. 145, p. 119843, Feb. 2026, doi: 10.1016/j.est.2025.119843.
[18] Senobar H. *et al.*, (2026) Phase change materials (PCMs) for thermal energy storage systems, *Materials Today Sustainability*, vol. 34, p. 101369, Jun. 2026, doi: 10.1016/j.mtsust.2026.101369.
[19] Samykano M., (2022) Role of phase change materials in thermal energy storage: Potential, recent progress and technical challenges, *Sustainable Energy Technologies and Assessments*, vol. 52, p. 102234, Aug. 2022, doi: 10.1016/j.seta.2022.102234.
[20] Irshad K. *et al.*, (2025) Experimental study and synergistic performance analysis of phase change material assisted cold thermal storage system for energy efficient air cooling, *Journal of Energy Storage*, vol. 108, p. 115018, Feb. 2025, doi: 10.1016/j.est.2024.115018.
[21] Han D., Guene Lougou B., Xu Y., huai Y. S, and Huang X., (2020) Thermal properties characterization of chloride salts/nanoparticles composite phase change material for high-temperature thermal energy storage, *Applied Energy*, vol. 264, p. 114674, Apr. 2020, doi: 10.1016/j.apenergy.2020.114674.
[22] Choo Y. M. and Wei W., (2022) Salt hydrates as phase change materials for photovoltaics thermal management, *Energy Science & Engineering*, vol. 10, no. 5, pp. 1630–1642, May 2022, doi: 10.1002/ese3.1007.
[23] Brancato V., Frazzica A., Sapienza A., and Freni A., (2017) Identification and characterization of promising phase change materials for solar cooling applications, *Solar Energy Materials and Solar Cells*, vol. 160, pp. 225–232, Feb. 2017, doi: 10.1016/j.solmat.2016.10.026.
[24] Pereira D C J. and Eames P., (2016) Thermal energy storage for low and medium temperature applications using phase change materials – A review, *Applied Energy*, vol. 177, pp. 227–238, Sep. 2016, doi: 10.1016/j.apenergy.2016.05.097.
[25] Oró E., De Gracia A., Castell A., Farid M. M., and Cabeza L. F., (2012) Review on phase change materials (PCMs) for cold thermal energy storage applications, *Applied Energy*, vol. 99, pp. 513–533, Nov. 2012, doi: 10.1016/j.apenergy.2012.03.058.
[26] Zhao C. Y., Lu W., and Tian Y., (2010) Heat transfer enhancement for thermal energy storage using metal foams embedded within phase change materials (PCMs), *Solar Energy*, vol. 84, no. 8, pp. 1402–1412, Aug. 2010, doi: 10.1016/j.solener.2010.04.022.
[27] Hirmiz R., Lightstone M. F., and Cotton J. S., (2018) Performance enhancement of solar absorption cooling systems using thermal energy storage with phase change materials, *Applied Energy*, vol. 223, pp. 11–29, Aug. 2018, doi: 10.1016/j.apenergy.2018.04.029.
[28] Farah S., Liu M., and Saman W., (2019) Numerical investigation of phase change material thermal storage for space cooling, *Applied Energy*, vol. 239, pp. 526–535, Apr. 2019, doi: 10.1016/j.apenergy.2019.01.197.
[29] Xie N., Huang Z., Luo Z., Gao X., Fang Y., and Zhang Z., (2017) Inorganic Salt Hydrate for Thermal Energy Storage, *Applied Sciences*, vol. 7, no. 12, p. 1317, Dec. 2017, doi: 10.3390/app7121317.
[30] Liu M., Li Z., Liu W., Liu Y., Wu X., and Xu C., (2025) Development of a PCM-Integrated Radiant Cold-Storage System: Radiative-Cooling Film, Water Tank Design, and Outdoor Performance Validation, *Energies*, vol. 18, no. 22, p. 5989, Nov. 2025, doi: 10.3390/en18225989.
[31] Li Z., Sha Y., and Zhang X., (2024) Research on Phase Change Cold Storage Materials and Innovative Applications in Air Conditioning Systems, *Energies*, vol. 17, no. 17, p. 4365, Aug. 2024, doi: 10.3390/en17174365.
[32] Liu J., Xiao Y., Chen D., Ye C., and Nie C., (2024) Melting and Solidification Characteristics of PCM in Oscillated Bundled-Tube Thermal Energy Storage System, *Energies*, vol. 17, no. 8, p. 1973, Apr. 2024, doi: 10.3390/en17081973.

[33] Jacob J. *et al.*, (2022) Quantifying thermophysical properties, characterization, and thermal cycle testing of nano-enhanced organic eutectic phase change materials for thermal energy storage applications, *Solar Energy Materials and Solar Cells*, vol. 248, p. 112008, Dec. 2022, doi: 10.1016/j.solmat.2022.112008.

[34] He M., Yang L., Lin W., Chen J., Mao X., and Ma Z., (2019) Preparation, thermal characterization and examination of phase change materials (PCMs) enhanced by carbon-based nanoparticles for solar thermal energy storage, *Journal of Energy Storage*, vol. 25, p. 100874, Oct. 2019, doi: 10.1016/j.est.2019.100874.

[35] Trigui A., Karkri M., Boudaya C., Candau Y., and Ibos L., (2013) Development and characterization of composite phase change material: Thermal conductivity and latent heat thermal energy storage, *Composites Part B: Engineering*, vol. 49, pp. 22–35, Jun. 2013, doi: 10.1016/j.compositesb.2013.01.007.

[36] Zhang S., Pu L., Xu L., Liu R., and Li Y., (2020) Melting performance analysis of phase change materials in different finned thermal energy storage, *Applied Thermal Engineering*, vol. 176, p. 115425, Jul. 2020, doi: 10.1016/j.applthermaleng.2020.115425.

[37] Yang T., King W. P., and Miljkovic N., (2021) Phase change material-based thermal energy storage, *Cell Reports Physical Science*, vol. 2, no. 8, p. 100540, Aug. 2021, doi: 10.1016/j.xcrp.2021.100540.

[38] Islam A., Pandey A. K., Saidur R., and Tyagi V. V., (2024) Shape stable composite phase change material with improved thermal conductivity for electrical-to-thermal energy conversion and storage, *Materials Today Sustainability*, vol. 25, p. 100678, Mar. 2024, doi: 10.1016/j.mtsust.2024.100678.

[39] Selvnes H., Allouche Y., Manescu R. I., and Hafner A., (2021) Review on cold thermal energy storage applied to refrigeration systems using phase change materials, *Thermal Science and Engineering Progress*, vol. 22, p. 100807, May 2021, doi: 10.1016/j.tsep.2020.100807.

[40] Rashid F. L. *et al.*, (2023) Recent Advances on The Applications of Phase Change Materials in Cold Thermal Energy Storage: A Critical Review, *J. Compos. Sci.*, vol. 7, no. 8, p. 338, Aug. 2023, doi: 10.3390/jcs7080338.

[41] Ukpe R. A. and Chokor A. A., (2022) Investigation of Heat Transfer Properties of Water-ethylene Glycol Mixture and some Commercial Coolants, *Applied Research Frontiers*, vol. 1, no. 1, Feb. 2022, doi: 10.36686/Ariviyal.ARF.2022.01.01.005.

[42] Gabas A. L., Telis-Romero J., and Telis V. R. N., (2003) Influence of Fluid Concentration on Freezing Point Depression and Thermal Conductivity of Frozen Orange Juice, *International Journal of Food Properties*, vol. 6, no. 3, pp. 543–556, Jan. 2003, doi: 10.1081/JFP-120021458.

[43] Bello E. T. *et al.*, (2025) Nano-coolants for thermal enhancement in heat exchangers: A review of prospects, challenges and applications, *Next Nanotechnology*, vol. 8, p. 100214, 2025, doi: 10.1016/j.nxnano.2025.100214.

[44] Yu K., Liu Y., Jia M., Wang C., and Yang Y., (2022) Thermal energy storage cement mortar containing encapsulated hydrated salt/fly ash cenosphere phase change material: Thermo-mechanical properties and energy saving analysis, *Journal of Energy Storage*, vol. 51, p. 104388, Jul. 2022, doi: 10.1016/j.est.2022.104388.

[45] Shao Y. L. *et al.*, (2020) Simulation and experimental study of thermal storage systems for district cooling system under commercial operating conditions, *Energy*, vol. 203, p. 117781, Jul. 2020, doi: 10.1016/j.energy.2020.117781.

[46] Alva V, Lin Y., Liu L., and Fang G., (2017) Synthesis, characterization and applications of microencapsulated phase change materials in thermal energy storage: A review, *Energy and Buildings*, vol. 144, pp. 276–294, Jun. 2017, doi: 10.1016/j.enbuild.2017.03.063.

[47] Gupta K. K. and Ramachandran M., (2018) Effect of Ethylene glycol as Phase Change Material in a Cold Storage Unit on retention of cooling, *IOP Conf. Ser.: Mater. Sci. Eng.*, vol. 377, p. 012190, Jun. 2018, doi: 10.1088/1757-899X/377/1/012190.

[48] Wang M., Zhang T., Zhou W., and Wang Y., (2026) Research on Thermal Performance and Structural Optimization of Finned Shell-and-Tube Storage Units for Air-Source Heat Pump Systems, *Buildings*, vol. 16, no. 5, p. 909, Feb. 2026, doi: 10.3390/buildings16050909.

[49] Karimi S. and Kwon S., (2021) Comparative analysis of the impact of energy-aware scheduling, renewable energy generation, and battery energy storage on production scheduling, *Int J Energy Res*, vol. 45, no. 13, pp. 18981–18998, Oct. 2021, doi: 10.1002/er.6999.

[50] Pourebrahim M. and Saboohi Y., (2026) Evaluation and reduction of heat transfer in buildings for energy storage using PCM - cooling and heating load diagram smoothing method, *Results in Engineering*, vol. 29, p. 108541, Mar. 2026, doi: 10.1016/j.rineng.2025.108541.

[51] Martínez-Ángeles M., Cabello R., Sánchez D., and Llopis R., (2025) Experimental evaluation and energy impact of a recuperative low-temperature heat exchanger in an autocascade system for ultra-low temperatures, *Applied Thermal Engineering*, vol. 276, p. 126978, Oct. 2025, doi: 10.1016/j.applthermaleng.2025.126978.

[52] Yan G., Liu Y., Qian Y., and Yu J., (2019) Theoretical study on a vapor compression refrigeration system with cold storage for freezer applications, *Applied Thermal Engineering*, vol. 160, p. 114091, Sep. 2019, doi: 10.1016/j.applthermaleng.2019.114091.

[53] Yang H., Li J., Ge Z., Yang L., and Du X., (2023) Dynamic performance for discharging process of pumped thermal electricity storage with reversible Brayton cycle, *Energy*, vol. 263, p. 125930, Jan. 2023, doi: 10.1016/j.energy.2022.125930.